Agar-based phantoms for skin diagnostic imaging

Kuzmina, Ilona, Lukinsone, Vanesa, Rubins, Uldis, Osina, Ilze, Dambite, Laura, et al.

Ilona Kuzmina, Vanesa Lukinsone, Uldis Rubins, Ilze Osina, Laura Dambite, Anna Maslobojeva, Janis Spigulis, "Agar-based phantoms for skin diagnostic imaging," Proc. SPIE 11363, Tissue Optics and Photonics, 113630F (2 April 2020); doi: 10.1117/12.2555674

SPIE.

Event: SPIE Photonics Europe, 2020, Online Only, France

Agar-based phantoms for skin diagnostic imaging

Ilona Kuzmina*, Vanesa Lukinsone, Uldis Rubins, Ilze Osina, Laura Dambite, Anna Maslobojeva, Janis Spigulis
Biophotonics Laboratory, Institute of Atomic Physics and Spectroscopy, University of Latvia, 19 Raina blvd., Riga, Latvia, LV-1050

ABSTRACT

Agar-based skin phantoms with different thicknesses and hemoglobin concentration were evaluated for diagnostics of skin lesions by RGB imaging. Scattering properties of the phantoms were simulated using intralipid, absorption properties – using lyophilized powder of human hemoglobin. RGB images of phantoms were captured by self-developed laboratory made devices. The algorithm for calculation of chromophore concentrations are based on Beer-Lambert law and includes the photon path length evaluated from the measured photon-time-of-flight signals. Optical properties and chromophore concentration maps of phantoms obtained from RGB images were analyzed. The influence of chromophore concentration on scattering and absorption, photon path length and chromophore maps are discussed.

Keywords: Skin optical phantoms, skin imaging, chromophore mapping, photon-time-of-flight, scattered photon path length, skin lesions.

1. INTRODUCTION

Tissue simulating phantoms are important for validation physical models and standardization of medical devices. Different kind of bulk materials can be used as a matrix of the phantoms with different absorbing and scattering substances to simulate tissue optical properties[1]. Agar-based phantoms are easy to produce semisolid hydrogels with index of refraction (n=1.35) close to the one of tissues (n=1.35-1.55)[2]. Hydrogel substance that are made from agar and water solution allows to mimic layers of skin. Stability of such phantoms are referred from some days to weeks[1,3]. Hydrogels have been used for studies of skin optical, mechanic, acoustic, surface and thermal properties. The stiffness of agar hydrogel depends on agar concentration and heating procedure. Different absorbing and scattering substances usually are added to simulate optical properties of the tissues[3]. The absorption and scattering of agar usually are neglected. However, Cook *et al*[4] observed the influence of gelatin concentration in phantom on scattering spectrum of Intralipid 20%. The authors observed that the scattering spectrum decreases with the increment of gelatin concentration that was explained by increment of refraction indices of matrix with the concentration of the gelatin. Intralipid is a lipid emulsion that is usually used for tissue scattering simulation in aqueous and hydrogel tissue phantoms. The size of lipid particles is in the range from 10 to 500nm, index of refraction – 1.45[1]. Chen et al[5] used agar combined with gelatin to produce dermis and hypodermis in multilayered agar phantoms for a study of skin mechanical, acoustic and optical properties, and intralipid (IL) as a scatter. Since the absorption of the melanin and hemoglobin are the most prominent in the skin, their optical properties are the most studied.

This paper presents agar-based phantoms for validation of the previously developed algorithm for concentration evaluation of skin chromophores. Here we compare the results obtained from RGB images captured by two self-developed smartphone-based prototypes and evaluate absorption properties of the phantoms using transmittance and diffuse reflectance images. In this paper, we also presented examples of hemoglobin concentration maps calculated by using experimentally determined photon mean free path values.

*ilona.kuzmina@lu.lv; phone 0037126448; asi.lv

Tissue Optics and Photonics, edited by Valery V. Tuchin, Walter C. P. M. Blondel, Zeev Zalevsky, Proc. of SPIE Vol. 11363, 113630F · © 2020 SPIE
CCC code: 0277-786X/20/$21 · doi: 10.1117/12.2555674

2. MATERIALS AND METHODS

2.1 Agar phantoms

Skin optical phantoms were produced using Agar (powder, A7002, Sigma-Aldrich), Intralipid (emulsion 20%, I141, Sigma-Aldrich), Hemoglobin (water soluble, 198285, Sigma-Aldrich). Agar hydrogel was made by mixing agar powder with tap water and heating of the solution. Intralipid (IL) were added to the solution for scattering simulation, hemoglobin (Hb) – for absorption simulation. Concentrations of Hb are presented in the table 1; concentration of intralipid of 1% was used in 3.3cm thick phantoms. The solutions were filled in cylindrical plastic forms with a diameter of ~5 cm and a height of 0.9-3.5cm. One-layer phantoms with different Hb concentrations with and without IL were made for determination of optical properties (absorption coefficient, photon path length) from images. The phantoms with thickness (h) of 3-3.5cm were prepared for measurements of the photon time-of-flight (PTOF) signals; 0.9 to 3.3 cm thick phantoms - for RGB imaging. Vascular neoplasms were simulated by adding some drops of Hb water (C_{Hb}=307μM) and Hb agar (C_{Hb}=6μM) solutions to the bulk agar phantom (matrix) with 1% intralipid to evaluate the concentration maps. The phantoms with simulated vascular vessels were made of two-layers of agar. The first (bottom) layer was 1cm thick with scratched channels where Hb water solution was filled; the second (top) layer was 2mm thick.

Table 1. Concentrations of hemoglobin (C_{Hb}) added to the one-layer phantoms.

C_{Hb}	
%	*μM*
0,5	1.5
1	3
2	6
3	9
3.5	10.5

2.2 Point spectral measurements

Steady state spectra of the phantoms were measured using broadband halogen lamp (AvaLight-Hal, Avantes BV), spectrometer (AvaSpec-Mini4096CL-UVI10, Avantes BV) in the spectral range 300-1100nm (Fig.1(a)). Diffuse reflectance spectra were measured using y-type reflectance probe (FCR-7UV400-2-ME, Avantes BV) with 6 illumination and one receiving fibers (400μm, UV/VIS). White reference tile WS2 (Avantes BV) was used as reference for reflectance measurements. Transmittance spectra were measured using illuminating fiber (600μm, UV/VIS, FC-UV600-2-ME, Avantes BV) and receiving fiber cable (7x200mm UV/VIS, round to linear type, FCRL-7UV200-2-ME, Avantes BV).

Phantom remitted photon propagation time (photon time-of-flight – PTOF) was measured by a TCSPC (time-correlated single photon counting) recording system using Fianium White-Laser-Micro with broad emission spectrum (400nm - 1000nm) as a light source. An experimental set-up is schematically shown in Fig.1(b). A wavelength of interest was selected by using interference filters. Point spectral measurements were performed at 520nm and 680nm and source-detector distance 1mm.

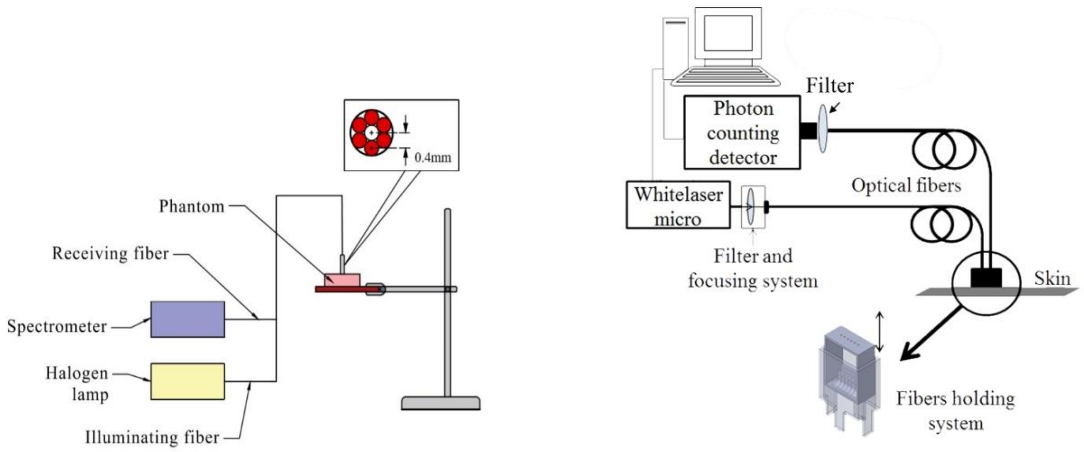

(a) (b)

Figure 1. Measurement schemes of diffuse reflectance spectra (a) and phantom remission kinetics[6] (b).

2.3 RGB imaging

RGB images of phantoms were captured by smartphone *Nexus5* with two add-on illuminators: set of RGB LEDs (*LED* prototype) and three wavelength laser illuminator (*Laser* prototype)[7–9]. *LED* prototype provides subsequent three-color illumination (intensity maxima of LEDs at 460nm, 535nm, 663nm), while *Laser* prototype provides simultaneous three laser line (448nm, 532nm, 659 nm) illumination that ensures single-snapshot mapping of the skin chromophores. A diameter of imaging area of both illuminators is 4cm; a distance between camera of *LED prototype* and the surface l=7cm, between camera of *Laser prototype* and the surface - l=8cm. Diffuse reflectance and transmittance RGB images were captured as shown in figure 1.

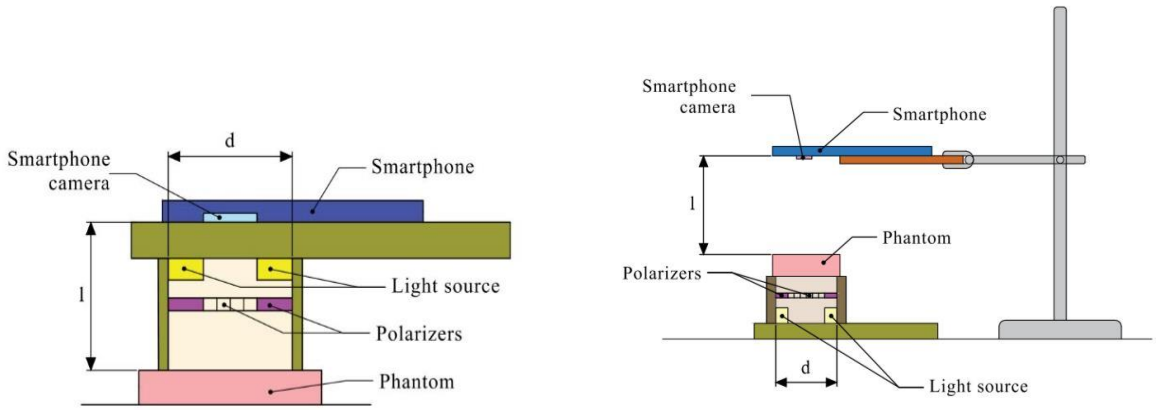

(a) (b)

Figure 2. Set-up of diffuse reflectance (a) and transmittance (b) measurements by smartphone prototypes.

2.4 Calculation of the phantoms' optical properties

Optical properties and hemoglobin concentration of the phantoms were calculated from RGB images using Beer-Lambert law. Absorption coefficients were calculated from transmittance and diffuse reflectance RGB images using equation:

$$I=I_0 \exp(-\mu_a \cdot l) \quad (1)$$

where I – intensity of transmitted or diffuse reflected light of a sample phantom, I_0 – intensity of transmitted or diffuse reflected light of a reference phantom, μ_a – absorption coefficient, l – thickness of the phantom layer (for transmittance

measurements) or photon mean path length (for reflectance measurements). Photon mean path length was calculated from measured PTOF signals. Detailed description of calculation is available elsewhere[6].

Chromophore concentration and extinction coefficients were calculated using equation:

$$\mu_a = 2.303 \cdot C \cdot \varepsilon \quad (2)$$

where C – concentration of the chromophore, ε – extinction coefficient.

The scheme of calculation of the chromophore concentrations is shown in fig.3.

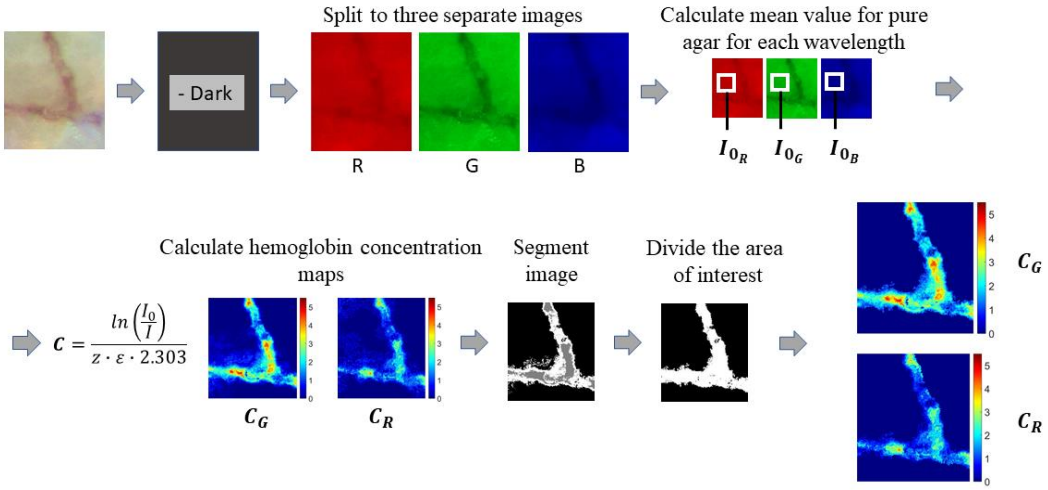

Figure 3. Functional scheme for calculation of the maps of chromophore concentrations. C_G – chromophore concentration map obtained from G image, C_R – chromophore concentration map obtained from R image.

3. RESULTS AND DISCUSSION

3.1 Optical properties of the phantoms

Figure 4 shows examples of skin optical phantoms. Diffuse reflectance spectra of the phantoms normalized to reference spectra are shown in figure 5. Absorption intensity increases with the concentration of the hemoglobin in phantom. Spectra normalized to white tile refence spectrum (Fig 5(a, c)) indicate water absorption in agar phantoms. For example, absorption peak at ~950nm can be explained by water absorption. Spectra normalized to the spectrum of pure agar phantom (Hb0%) show absorption peaks at ~414nm and ~536nm for Hb phantoms.

Figures 6-9 show optical properties of the phantoms calculated from transmittance and diffuse reflectance RGB images. Figure 6 illustrate a dependence of absorption coefficients obtained from transmittance images on hemoglobin concentration added to the phantoms of three different thicknesses (0.9cm, 1.5cm, 3.3cm). The absorption increases with the increment of concentration. In most of the cases the highest values are observed for images captured under “blue” illumination (at 460nm and 448nm), the lowest – under “red” illumination (at 660nm and 663nm). The exception are thick phantoms (~3.3cm), where blue light was strongly absorbed, and it wasn’t possible to evaluate absorption from dark images (Fig.6(e)).

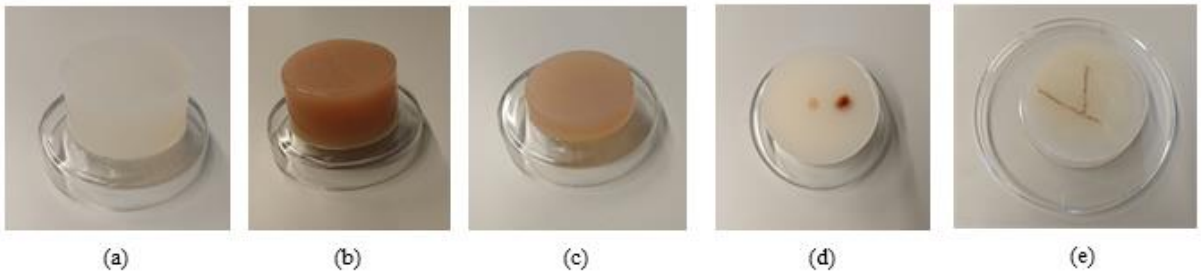

Figure 4. Examples skin optical phantoms: pure agar phantom with thickness (h) of 3.3cm (a), phantom with Hb (3%) and IL (1%) h=3.3cm (b), phantom with Hb (1%) h=1.5cm (c), phantom with simulated vascular neoplasms h=3.5cm (d), two-layered phantoms with simulated vascular vessel (e).

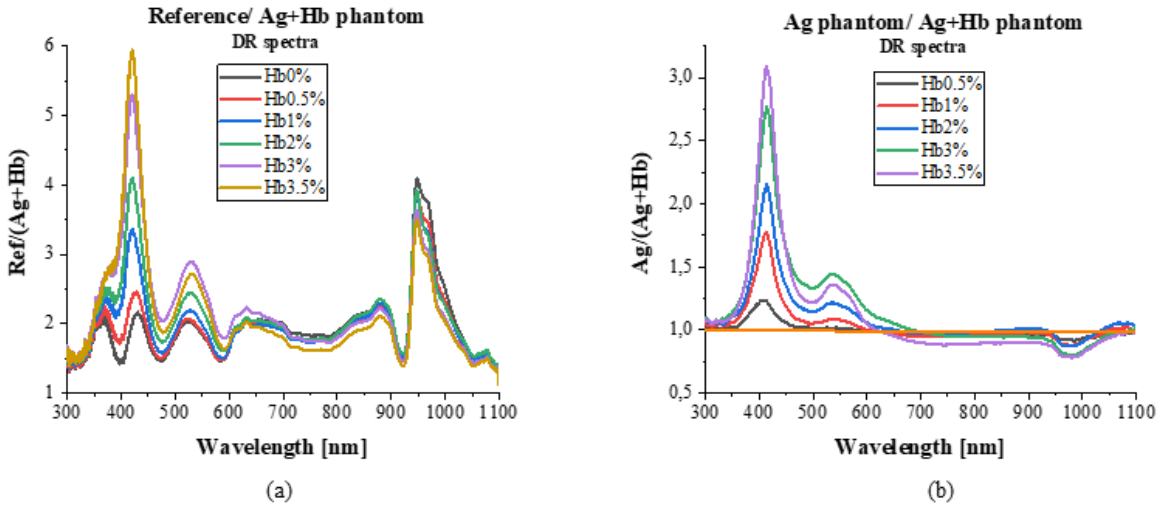

Figure 5. Diffuse reflectance spectra of Hb with thickness h=1.5cm normalized to reference spectra obtained from white reference tile (a) and agar phantom without Hb (b).

Figure 7 compares extinction coefficients achieved from the "green" and "red" images of the phantoms with different thicknesses. It is expected that the values of extinction coefficient should remain the same at different Hb concentration in the phantom. The results show the less fluctuations of the values for images captured by *Laser* prototype at 660nm. Coefficients obtained from *Laser* prototype have the highest values for the phantoms with the thickness 0.9cm. Values decrease with increasing of phantom thickness.

Figure8 compares mean values of Hb extinction coefficient obtained by the LED and Laser prototypes with the values obtained by other authors[10]. Figure 8 (a, b, c) show the results calculated from transmittance images for three different thicknesses of the phantoms, figure 8(d) – from diffuse reflectance images for 3.3cm thick phantoms. Extinction coefficients calculated from transmittance images are higher compared to the values obtained by other authors[10]. The less changes of the extinction coefficient over the concentration was observed for *Laser* prototype at wavelength 660nm. Diffuse reflectance images were captured only from thick phantoms (h=3.3cm) to eliminate the reflection from the background. The photon mean pathlength was obtained from experimentally measured PTOF signals at 520nm and 680nm (table 2). It was used for extinction coefficient calculation from diffuse reflectance images. Obtained values are closer to the values of deoxyhemoglobin compared to transmittance images. Results obtained by *Laser* prototype are more precise compared to the results obtained by *LED* prototype.

Table 2. Photon mean pathlength (MPL) obtained from measured PTOF signals on phantoms with Hb and IL (C_{IL}=1%) at 1mm distance of the source-detector fiber.

Wavelength, nm	MPL, mm	
	C_{Hb}=1%	C_{Hb}=2%
520	14.9	16.1
680	18.9	21.1

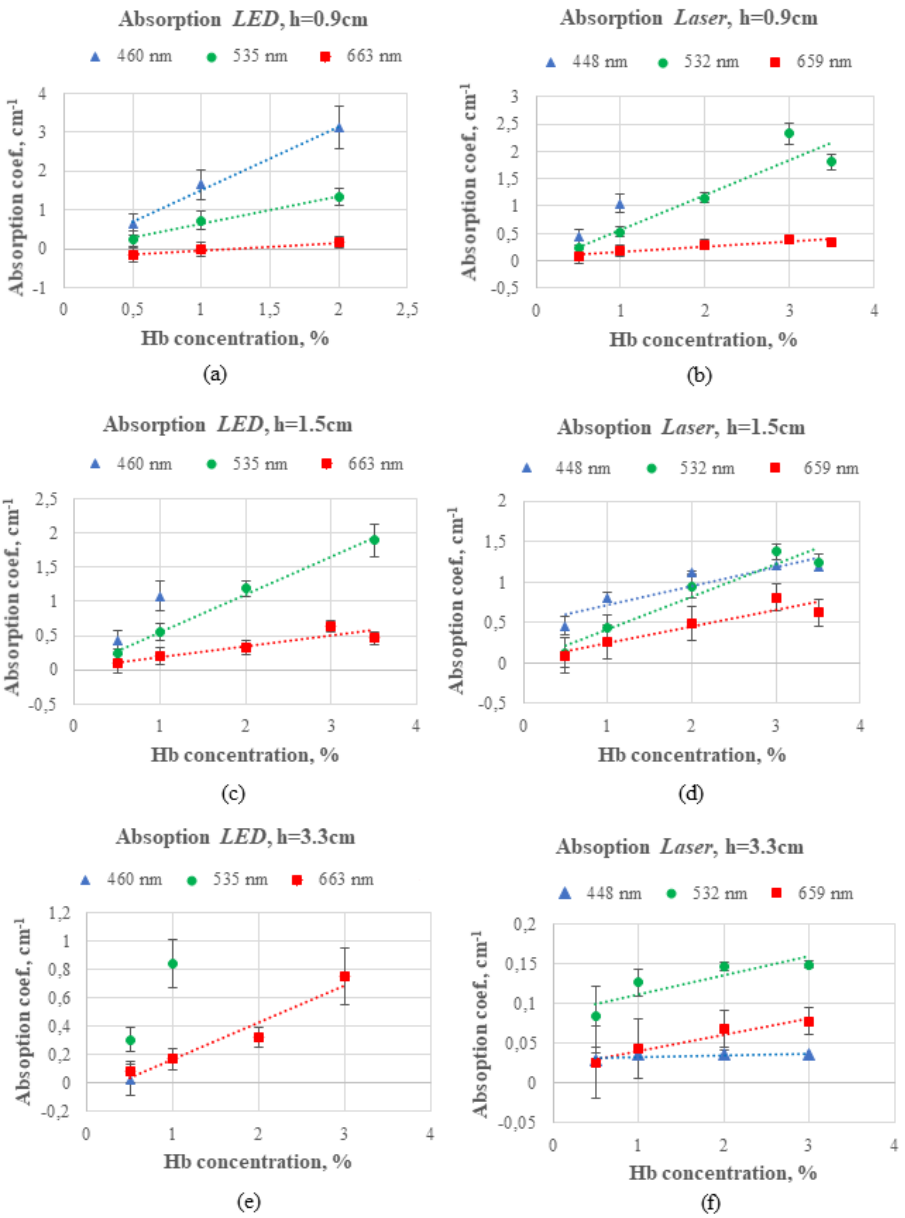

Figure 6. Dependence of Hb absorption coefficient calculated from RGB images of the LED and Laser devices on Hb concentration for three different thicknesses (h) of the phantoms.

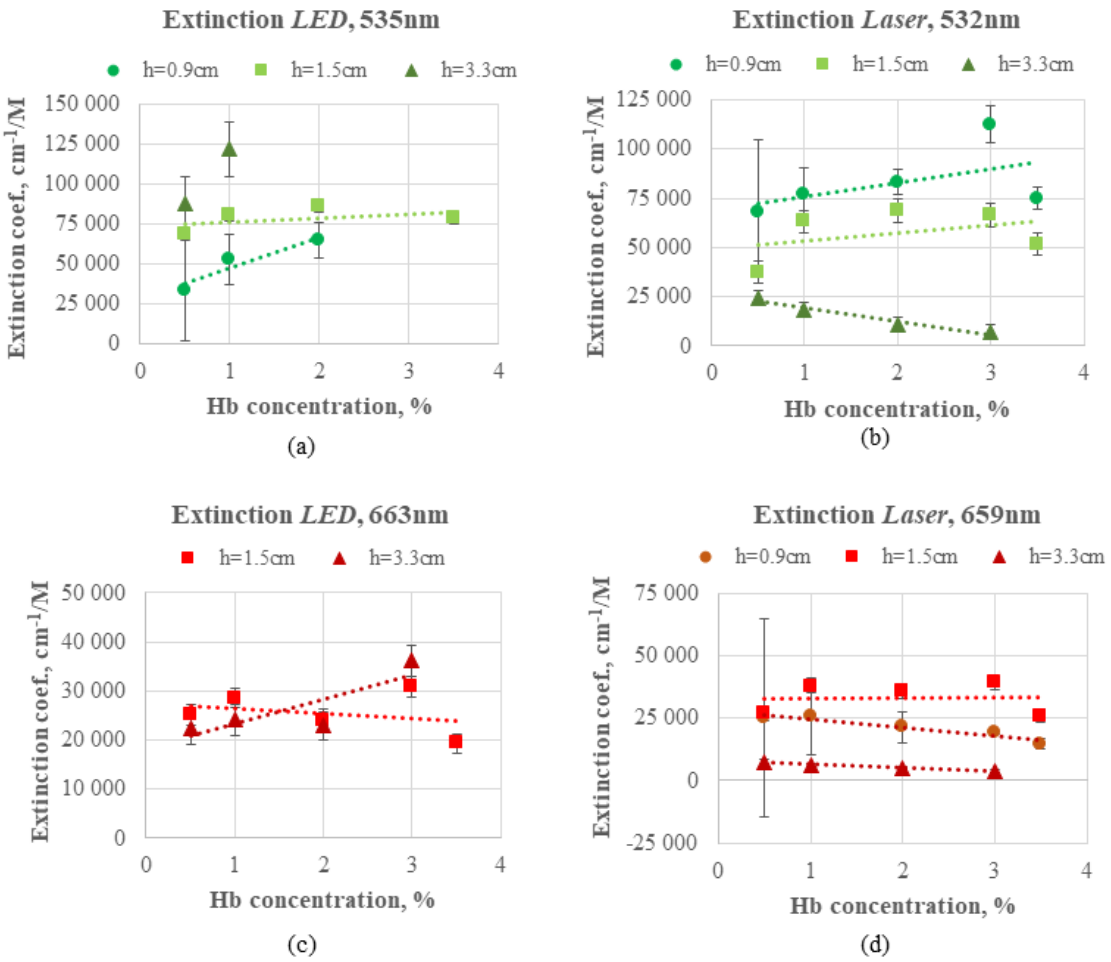

Figure 7. Dependence of Hb extinction coefficient calculated from RGB images of LED and Laser devices on Hb concentration for three different thicknesses (h) of the phantoms.

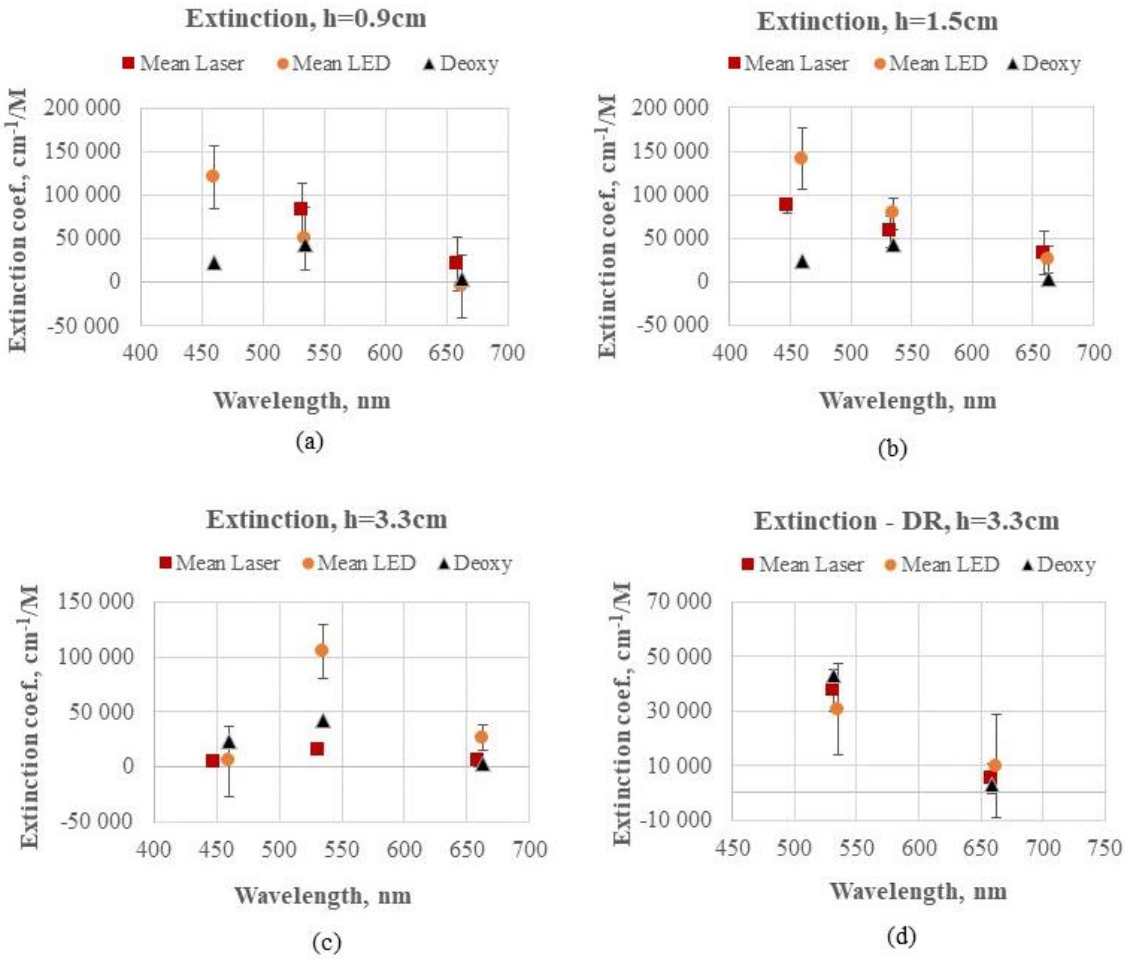

Figure 8. Spectral dependence of the mean values of extinction coefficient calculated from transmittance (a, b, c) and diffuse reflectance (d) RGB images of Hb phantoms captured by LED and Laser prototypes compared with values of deoxyhemoglobin (Deoxy) obtained by other authors[10]. h – thickness of the phantoms.

3.2 Hemoglobin concentration maps

Diffuse reflectance RGB images of simulated skin vascular vessels and neoplasms with corresponding chromophore maps (calculated from images captured under green and red illumination) are shown in figures 9-11. In all three figures the distribution of Hb concentration is slightly different in G and R maps which can be explained by different penetration depth of "green" and "red" illumination. The concentrations in the maps also differs from the concentration of added solutions. For example, the calculated Hb concentration of simulated neoplasm of the added Hb water solution (C_{Hb}=307μM) does not exceed 15μM (Fig.11 (b, c)), concentration of Hb agar solution (C_{Hb}=6μM) does not exceed the value of 3μM (Fig.10 (b, c)). It can be explained by the fact that during the solidification of the phantom the added hemoglobin solution can partially diffuse and mix with the bulk material.

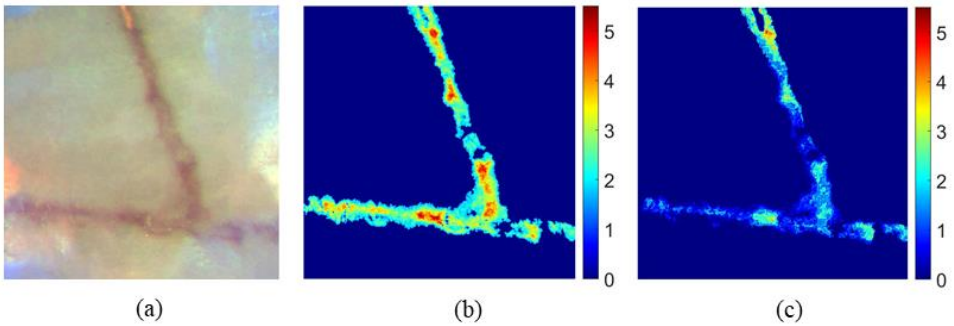

Figure 9. RGB image (a) and Hb concentration maps of the two-layered phantom with simulated vascular vessel (Hb water solution, C_{Hb}=307μM) obtained from G (b) and R (c) images (*LED* prototype). The "jet" scale indicates the concentration in μM.

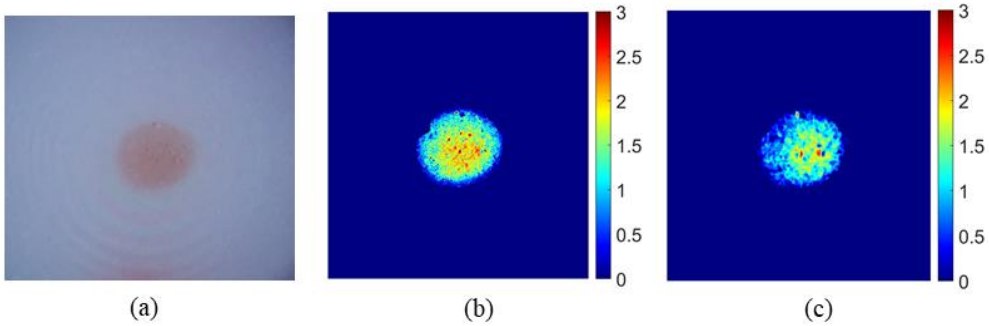

Figure 10. RGB image (a) and Hb concentration maps of the phantom with simulated neoplasm (Hb agar solution, C_{Hb}=6μM) obtained from G (b) and R (c) images (*Laser* prototype). The "jet" scale indicates the concentration in μM.

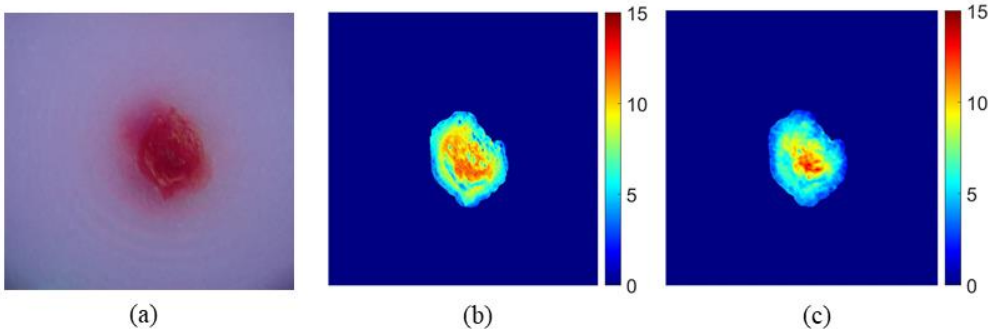

Figure 11. RGB image (a) and Hb concentration maps of the phantom with simulated neoplasm (Hb water solution, C_{Hb}=307μM) obtained from G (b) and R (c) images (*Laser* prototype). The "jet" scale indicates the concentration in μM.

4. CONCLUSIONS

In this work, we presented agar-based phantoms for evaluation and mapping of the hemoglobin concentration by RGB imaging. We compared two smartphone-based Laser and LED devices and two measurement techniques: transmittance and diffuse reflectance imaging. We also presented the hemoglobin concentration maps of the phantoms obtained by using the experimentally measured photon time of flight signals. The values of extinction coefficients from diffuse reflectance images were closer to the values obtained by other authors compared to transmission images. The images captured by *Laser* prototype showed more precise results compared to the *LED* prototype.

ACKNOWLEDGEMENTS

This work has been supported by European Regional Development Fund project 'Multimodal imaging technology for in-vivo diagnostics of skin malformations' under grant agreement #1.1.1.1/18/A/132.

REFERENCES

[1] Pogue, B. W. and Patterson, M. S., "Review of tissue simulating phantoms for optical spectroscopy, imaging and dosimetry," J. Biomed. Opt. **11**(4), 041102 (2006).

[2] Bolin, F. P., Preuss, L. E., Taylor, R. C. and Ference, R. J., "Refractive index of some mammalian tissues using a fiber optic cladding method," Appl. Opt. **28**(12), 2297 (1989).

[3] Dabrowska, A. K., Rotaru, G. M., Derler, S., Spano, F., Camenzind, M., Annaheim, S., Stämpfli, R., Schmid, M. and Rossi, R. M., "Materials used to simulate physical properties of human skin," Ski. Res. Technol. **22**(1), 3–14 (2016).

[4] Cook, J. R., Bouchard, R. R. and Emelianov, S. Y., "Tissue-mimicking phantoms for photoacoustic and ultrasonic imaging," Biomed. Opt. Express **2**(11), 3193 (2011).

[5] Chen, A. I., Balter, M. L., Chen, M. I., Gross, D., Alam, S. K., Maguire, T. J. and Yarmush, M. L., "Multilayered tissue mimicking skin and vessel phantoms with tunable mechanical, optical, and acoustic properties," Med. Phys. **43**(6), 3117–3131 (2016).

[6] Lukinsone, V., Osis, M., Latvels, J., Kuzmina, I., Rubins, U., Zorina, N., Maslobojeva, A. and Spigulis, J., "Towards direct measurements of remitted photon path lengths in skin: kinetic studies in the range 520-800 nm," Nov. Biophotonics Tech. Appl. V **1107505**(July), 4 (2019).

[7] Kuzmina, I., Lacis, M., Spigulis, J., Berzina, A. and Valeine, L., "Study of smartphone suitability for mapping of skin chromophores," J. Biomed. Opt. **20**(9), 090503 (2015).

[8] Spigulis, J. and Oshina, I., "Snapshot RGB mapping of skin melanin and hemoglobin," J. Biomed. Opt. **20**(5), 050503 (2015).

[9] Spigulis, J., "Multispectral, Fluorescent and Photoplethysmographic Imaging for Remote Skin Assessment," Sensors **17**(5), 1165 (2017).

[10] Prahl, S., "Optical Absorption of Hemoglobin," Oregon Med. Laser Cent., 1999, <https://omlc.org/spectra/hemoglobin/> (12 August 2018).